

## Control Lyapunov Function for Controllable Series Devices

M. Ghandhari\*

G. Andersson\*\*

I. A. Hiskens

Royal Institute of Technology (KTH)  
Sweden

University of Illinois  
USA

### Summary

Power systems exhibit various modes of oscillation due to interactions among system components. Many of the oscillations are due to synchronous machine rotors swinging relative to each other.

Controllable Series Devices (CSD), i.e. series connected Flexible AC Transmission Systems (FACTS) devices, such as Unified Power Flow Controller (UPFC), Controllable Series Capacitor (CSC) and Quadrature Boosting Transformer (QBT) offer a means to mitigate power system oscillations. For these devices, a general model which is referred to as injection model is used. Having a CSD between buses  $\mathbf{i}$  and  $\mathbf{j}$ , then powers between these buses are given by

$$\begin{aligned} P_{ij} &= P_{ij}^o + P_{si} & , & & P_{ji} &= P_{ji}^o + P_{sj} \\ Q_{ij} &= Q_{ij}^o + Q_{si} & , & & Q_{ji} &= Q_{ji}^o + Q_{sj} \end{aligned}$$

where  $P_s$  and  $Q_s$  are contributions of the CSD which are controllable.  $P^o$  and  $Q^o$  are the powers between the buses  $\mathbf{i}$  and  $\mathbf{j}$  in the absence of a CSD.

The CSD with a suitable control scheme can improve transient stability and help to damp electromechanical oscillations. Therefore, a question of great importance is the selection of the input signals and a control law for these devices in order to damp power oscillations in an effective and robust manner. This paper develops a control strategy for the CSD based on Control Lyapunov Function (CLF). Lyapunov theory deals with dynamical systems without inputs. For this reason, it has traditionally been applied only to closed loop control systems, that is, systems for which the input has been eliminated through the substitution of a predetermined feedback control. However some authors started using Lyapunov function candidates in feedback design itself by making the Lyapunov derivative negative when choosing the control. Such ideas have been made

precise with the introduction of the concept of a CLF for systems with control input. Now, Consider the affine system

$$\dot{x} = f(x, u) = f_c(x) + \sum_{i=1}^m u_i f_i(x)$$

we want to find a feedback control  $u = u(x)$  such that the closed-loop system  $\dot{x} = f(x, u(x))$  has a locally asymptotically stable equilibrium point at the origin, i.e.  $f(0, u(0)) = 0$ . According to the Jurdjevic-Quinn approach, if there exists a positive definite function  $\mathcal{V}(x)$  such that  $\text{grad}(\mathcal{V}) \cdot f_c(x) \leq 0$ , then a stabilising feedback law is typically defined for  $i = 1 \dots m$ , by

$$u_i(x) = -\text{grad}(\mathcal{V}) \cdot f_i(x)$$

Thus, the time derivative of  $\mathcal{V}(x)$  with respect to the closed-loop system is given by

$$\dot{\mathcal{V}}(x) = \text{grad}(\mathcal{V}) \cdot f_c(x) - \sum_{i=1}^m (\text{grad}(\mathcal{V}) \cdot f_i(x))^2 \leq 0$$

For power systems without control input, i.e. without CSD, it can be shown that there exists a positive function  $\mathcal{V}(x)$ , which is known as energy function, such that

$\dot{\mathcal{V}} = \dot{\mathcal{V}}_{\text{NOCSD}} \leq 0$ . Using  $\mathcal{V}(x)$  as a Lyapunov function for the power systems with CSD between buses  $\mathbf{i}$  and  $\mathbf{j}$ , then we have

$$\dot{\mathcal{V}} = \dot{\mathcal{V}}_{\text{NOCSD}} + \dot{\mathcal{V}}_{\text{CSD}} \leq \dot{\mathcal{V}}_{\text{CSD}}$$

where

$$\dot{\mathcal{V}}_{\text{CSD}} = -P_{si} \dot{\theta}_i - P_{sj} \dot{\theta}_j - Q_{si} \frac{\dot{V}_i}{V_i} - Q_{sj} \frac{\dot{V}_j}{V_j}$$

which is controllable to be made negative.  $V$  and  $\theta$  are voltage and phase at bus  $\mathbf{i}$  ( and  $\mathbf{j}$  ), respectively.

**Keywords:** FACTS, UPFC, QBT, CSC and CLF

\* Dept. of Electric Power Engineering, Royal Institute of Technology (KTH), S-100 44 Stockholm, Sweden  
E-mail: [Mehrdad.Ghandhari@ekc.kth.se](mailto:Mehrdad.Ghandhari@ekc.kth.se)

\*\* Present address: Dept. of Electrical Engineering, ETL G26, Federal Institute of Technology (ETH), CH-8092 Zürich, Switzerland

**Abstract-** Controllable Series Devices (CSD), i.e. series connected Flexible AC Transmission Systems (FACTS) devices, such as Unified Power Controller (UPFC), Controllable Series Capacitor (CSC) and Quadrature Boosting Transformer (QBT) with a suitable control scheme can improve transient stability and help to damp electromechanical oscillations. For these devices, a general model, which is referred to as injection model, is used. This model is valid for load flow and angle stability analysis and is helpful for understanding the impact of the CSD on power system stability. Also, based on Lyapunov theory a control strategy for damping of electromechanical power oscillations in a multi-machine power system is derived. Lyapunov theory deals with dynamical systems without inputs. For this reason, it has traditionally been applied only to closed loop control systems, that is, systems for which the input has been eliminated through the substitution of a predetermined feedback control. However, in this paper, we use Lyapunov function candidates in feedback design itself by making the Lyapunov derivative negative when choosing the control. This control strategy is called Control Lyapunov Function (CLF) for systems with control inputs.

## 1. INTRODUCTION

Power systems exhibit various modes of oscillation due to interactions among system components. Many of the oscillations are due to synchronous machine rotors swinging relative to each other. In this paper, the electromechanical oscillations (initiated by faults) which typically are in the frequency range of 0.1 to 2 Hz, are considered.

In recent years, the fast progress in the field of power electronics has opened new opportunities for the power industry via utilization of the Controllable Series Devices (CSD), such as Unified Power Controller (UPFC), Controllable Series Capacitor (CSC) and Quadrature Boosting Transformer (QBT) which offer a new means to mitigate power system oscillations. Thus, a question of great importance is the selection of the input signals and a control strategy for these devices in order to damp power oscillations in an effective and robust manner.

Modern power systems are large scale and complex. Disturbances typically change the network topology and result in nonlinear system response. Also, because of deregulation the configuration of the interconnected grid will routinely be in a state of change. Therefore a control strategy that will counteract a wide variety of disturbances that may occur in the power system is attractive. This paper develops a control strategy for the CSD, based on the Control Lyapunov Function (CLF). The derived control strategy has the same basic structure for all CSD and it is based on input signals that easily can be obtained from locally measurable variables.

This paper is organized as follows. In Section 2 modeling of the CSD based on the injection model is presented. Section 3 describes the ideas with CLF and its application in power system. Also, a control strategy for the CSD is developed based on the CLF. We provide

some numerical test results, discussions and the conclusions of this paper in Sections 4, 5 and 6, respectively.

## 2. INJECTION MODEL

Fig. 1 shows the equivalent circuit diagram of a CSD which is located between buses **i** and **j**. UPFC and QBT inject a voltage in series with transmission line through a series transformer. The active power involved in the series injection is taken from the transmission line through a shunt transformer. UPFC generates or absorbs the needed reactive power locally by the switching operation of its converters [1], while the reactive power injected in series with the transmission line by the QBT, is taken from the transmission line and is circulated through the shunt transformer. For UPFC and QBT,  $x_s$  is the effective reactance seen from the transmission line side of the series transformer.  $\bar{V}_{se}$  is the injected series voltage source and  $\bar{I}_{sh}$  represents a current source. The reactive power delivered or absorbed by current source is independently controllable by the UPFC.

A CSC can be considered as a controllable reactance  $x_c$  which is connected in series with the transmission line. Thus, Fig. 1 is also valid for CSC when  $\bar{I}_{sh}$  is set to zero,  $\bar{V}_{se} = -jx_c \bar{I}_{ij}$  and  $x_s$  is the transmission line reactance  $x_L$ .

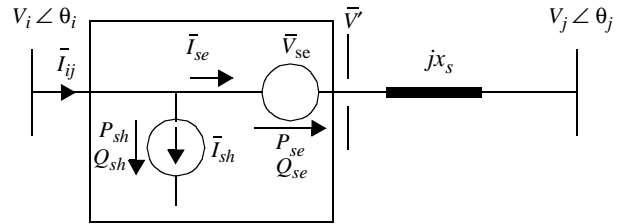


Fig. 1: Equivalent circuit diagram of a CSD

Fig. 2 shows the vector diagram of the equivalent circuit diagram of the CSD.

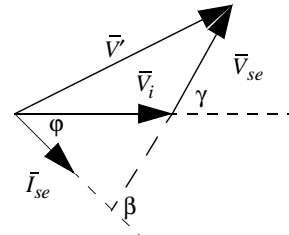


Fig. 2: Vector diagram of the CSD

For UPFC and QBT, the series voltage source is controllable in magnitude and phase, i.e.

$$\bar{V}_{se} = r \bar{V}_i e^{j\gamma} \quad (1)$$

where  $0 \leq \gamma \leq 2\pi$  for UPFC,  $\gamma = \pm \frac{\pi}{2}$  for QBT and

for both devices  $0 \leq r \leq r_{\max}$ . For CSC,  $\beta = \frac{\pi}{2}$ .

The injection model is obtained by replacing the series

voltage source by a current source  $\bar{I}_{inj} = -jb_s \bar{V}_{se}$  in parallel with the series reactance where  $b_s = 1/x_s$ .

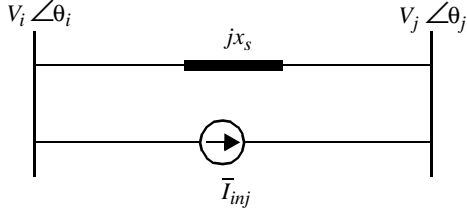


Fig. 3: Replacement of  $\bar{V}_{se}$  by  $\bar{I}_{inj}$

For UPFC and QBT, the current source corresponds to the injection powers  $S_i$  and  $S_j$ , i.e.

$$\begin{aligned}\bar{S}_i &= \bar{V}_i (-\bar{I}_{inj})^* = -(P_i + jQ_i) \\ &= -(rb_s V_i^2 \sin \gamma + jrb_s V_i^2 \cos \gamma) \\ \bar{S}_j &= \bar{V}_j (\bar{I}_{inj})^* = -(P_j + jQ_j) \\ &= rb_s V_i V_j \sin(\theta_{ij} + \gamma) + jrb_s V_i V_j \cos(\theta_{ij} + \gamma)\end{aligned}$$

where  $\theta_{ij} = \theta_i - \theta_j$ .

Thus, the injection model of the series part of these devices can be considered as shown in Fig. 4.

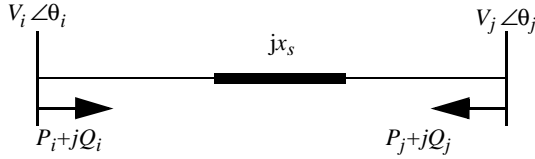


Fig. 4: Injection model of the series part

The apparent power supplied by the series voltage source is calculated from:

$$\bar{S}_{se} = \bar{V}_{se} (\bar{I}_{se})^* = jb_s r e^{j\gamma} \bar{V}_i (\bar{V}' - \bar{V}_j)^*$$

Active and reactive powers supplied by the series voltage source are distinguished as:

$$P_{se} = rb_s V_i V_j \sin(\theta_{ij} + \gamma) - rb_s V_i^2 \sin \gamma$$

$$Q_{se} = -rb_s V_i V_j \cos(\theta_{ij} + \gamma) + rb_s V_i^2 \cos \gamma + r^2 b_s V_i^2$$

For both UPFC and QBT in which losses are neglected,  $P_{sh} = P_{se}$ . For QBT,  $Q_{sh} = Q_{se}$ . For UPFC,  $Q_{sh}$  is independently controllable and we assume that it is zero. Note that  $Q_{sh}$  can also have a nonzero value.

The injection model for UPFC and QBT is constructed by adding  $P_{sh} + jQ_{sh}$  to bus  $i$  in Fig. 4.

An injection model for CSC can also be derived based on Fig. 3.

The injection model for the CSD is shown in Fig. 5.

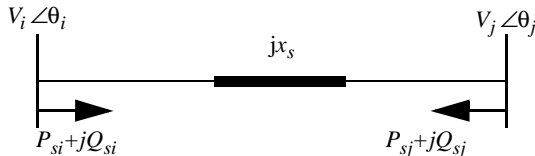


Fig. 5: Injection model for the CSD

In Fig. 5, for

**UPFC:**

$$P_{si} = b_s V_i V_j (u_1 \sin \theta_{ij} + u_2 \cos \theta_{ij}) \quad Q_{si} = u_1 b_s V_i^2$$

$$P_{sj} = -P_{si} \quad Q_{sj} = -b_s V_i V_j (u_1 \cos \theta_{ij} - u_2 \sin \theta_{ij})$$

where  $u_1 = r \cos \gamma$  and  $u_2 = r \sin \gamma$ . Note that

$$r = \sqrt{u_1^2 + u_2^2} \quad \text{and} \quad \gamma = \arctan\left(\frac{u_2}{u_1}\right).$$

**QBT:**

$$P_{si} = ub_s V_i V_j \cos \theta_{ij} \quad Q_{si} = u^2 b_s V_i^2 + ub_s V_i V_j \sin \theta_{ij}$$

$$P_{sj} = -P_{si} \quad Q_{sj} = ub_s V_i V_j \sin \theta_{ij}$$

where  $u = r \sin \gamma$  and  $-r_{\max} \leq u \leq r_{\max}$ . Obviously,

$$r = |u| \quad \text{and} \quad \gamma = \text{sign}(u) \frac{\pi}{2}, \quad \text{since} \quad \gamma = \pm \frac{\pi}{2}.$$

**CSC:**

$$P_{si} = u c_b V_i V_j \sin \theta_{ij} \quad Q_{si} = u c_b (V_i^2 - V_i V_j \cos \theta_{ij})$$

$$P_{sj} = -P_{si} \quad Q_{sj} = u c_b (V_j^2 - V_i V_j \cos \theta_{ij})$$

where

$$u_c = \frac{x_c}{x_L - x_c}, \quad x_{c\min} \leq u_c \leq x_{c\max} \quad (2)$$

### 3. CONTROL LYAPUNOV FUNCTION

#### 3.1 THEORETICAL CONSIDERATION

Power systems are most naturally described by Differential Algebraic (DA) models of the form  $\dot{x} = f(x, y)$  and  $0 = g(x, y)$ . The algebraic states  $y$  are related to the dynamic states  $x$  through the algebraic equations  $g$ . By virtue of the implicit function theorem, it can be shown that this model is locally equivalent to a differential equation model

$$\dot{x} = f(x, h(x)) = \tilde{f}(x), \quad x \in \Omega \in \mathbb{R}^n \quad (3)$$

if  $\frac{\partial g}{\partial y}$  is nonsingular. Under certain modeling assumptions, e.g., constant admittance loads, local equivalence extends to global equivalence. This model has become known in the energy function literature as the Reduced Network Model (RNM) [8]. The presentation of Control Lyapunov Function (CLF) in this paper is based on (3). Most ideas extend naturally to the DA model though.

Let the origin be an equilibrium point of system (3), i.e.  $\tilde{f}(0) = 0$ , possibly after a coordinate change. A function  $\mathcal{V}(x)$  is said to be a Lyapunov function for (3), if it is of class (at least)  $C^1$  and there exists a neighborhood  $\mathcal{Q}$  of the origin such that

$$\mathcal{V}(x) > 0, \quad \forall x \in \mathcal{Q}, \quad x \neq 0 \quad \text{and} \quad \mathcal{V}(0) = 0 \quad (4)$$

$$\dot{\mathcal{V}}(x) < 0, \quad \forall x \in \mathcal{Q}, \quad x \neq 0 \quad \text{and} \quad \dot{\mathcal{V}}(0) = 0 \quad (5)$$

If (3) has a Lyapunov function then the origin is locally asymptotically stable. Conversely, for any locally asymptotically stable system, a Lyapunov function exists.

For mechanical and electrical systems, the physical

energy (or energy-like) functions are often used as Lyapunov function candidates. The time derivatives of these energy functions are negative semidefinite. Therefore, these functions fail to satisfy condition (5) for Lyapunov function. However, applying La Salle's invariance principle or the theorems of Barbashin and Krasovskii [2], the energy functions satisfy the asymptotic stability condition and they can be considered as Lyapunov function candidates.

Lyapunov theory deals with dynamical systems without inputs. For this reason, it has traditionally been applied only to closed loop control systems, that is, systems for which the input has been eliminated through the substitution of a predetermined feedback control. However, some authors, [3]-[4], started using Lyapunov function candidates in feedback design itself by making the Lyapunov derivative negative when choosing the control. Such ideas have been made precise with the introduction of the concept of a Control Lyapunov Function for systems with control input [5].

The following discussion largely follows that in [6] and references therein. Consider the control system

$$\dot{x} = f(x, u), \quad x \in \Omega \in \mathbb{R}^n, \quad u \in \mathbb{R}^m \quad (6)$$

We want to find conditions for the existence of a feedback control  $u = u(x)$  defined in a neighborhood of the origin such that the closed-loop system  $\dot{x} = f(x, u(x))$  has a locally asymptotically stable equilibrium point at the origin, i.e.  $f(0, u(0)) = 0$ . If such a function  $u(x)$  exists, we say that (6) is stabilizable at the origin and the function  $u(x)$  is called a stabilizing feedback law or a stabilizer. Assume that (6) is continuously stabilizable. According to the Converse Lyapunov's Theorems [2], there must be a positive definite function  $\mathcal{V}(x)$  such that

$$\dot{\mathcal{V}}(x) = \text{grad}(\mathcal{V}) \cdot f(x, u(x)) < 0, \quad \forall x \in Q, \quad x \neq 0 \quad (7)$$

A function  $\mathcal{V}(x)$  satisfying (4) and (7) is called CLF.

Next, consider the affine system

$$\dot{x} = f(x, u) = f_c(x) + \sum_{i=1}^m u_i f_i(x) \quad (8)$$

where  $f_c(x)$  is the system without control. For sake of simplicity, we assume  $f_c(0) = 0$ , so that we can take also  $u_i(0) = 0$ . In [3], Artstein proved that there exists a stabilizer  $u_i(x)$  for (8), if and only if (8) admits a CLF.

In [4], Sontag presented explicit formulas for  $u_i(x)$ . In the case of using an energy function as a Lyapunov function candidate, the treatment of system (8) fits better in the framework of the Jurdjevic-Quinn approach [7]. We say that (8) satisfies a Lyapunov condition of the Jurdjevic-Quinn type if there is a neighborhood  $Q$  of the origin and a  $C^\infty$  function  $\mathcal{V}(x)$  such that (4) holds and  $\text{grad}(\mathcal{V}) \cdot f_c(x) \leq 0$  for  $x \in Q$ . According to the Jurdjevic-Quinn approach, a stabilizing feedback law is typically defined componentwise for  $i = 1 \dots m$  by  $u_i(x) = -\text{grad}(\mathcal{V}) \cdot f_i(x)$ . Thus, the time derivative of

$\mathcal{V}(x)$  for  $x \in Q$  with respect to the closed-loop system is given by

$$\begin{aligned} \dot{\mathcal{V}}(x) &= \text{grad}(\mathcal{V}) \cdot f_c(x) + \sum_{i=1}^m u_i f_i(x) \leq \sum_{i=1}^m u_i f_i(x) = \\ &= -\sum_{i=1}^m (\text{grad}(\mathcal{V}) \cdot f_i(x))^2 < 0 \end{aligned} \quad (9)$$

since  $\text{grad}(\mathcal{V}) \cdot f_c(x) \leq 0$ .

**Example:**

Consider the Single Machine Infinite Bus (SMIB) system shown in Fig. 6.

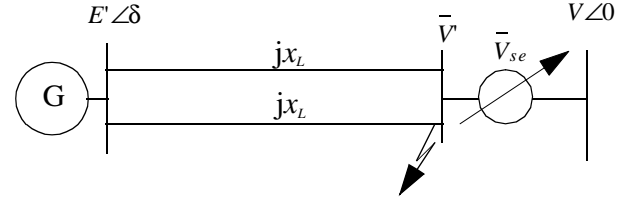


Fig. 6: A SMIB system

The post fault dynamics of this system without CSD, i.e.  $\bar{V}_{se} = 0$ , are given by

$$\begin{aligned} \dot{\delta} &= \omega - \omega_s \\ \dot{\omega} &= (P_m - P_e - D(\omega - \omega_s)) / M \end{aligned} \quad (10)$$

where  $D \geq 0$ ,  $P_e = bE'V \sin \delta$  and  $b = 1/x_L$ .

Let  $x = [\delta \quad \omega]^T$  and consider (10) as  $\dot{x} = f_c(x)$ . For system (10), the following energy function exists [8]

$$\mathcal{V} = \frac{1}{2} M (\omega - \omega_s)^2 - P_m \delta - bE'V \cos \delta + C_s \quad (11)$$

where  $C_s$  is a constant such that  $\mathcal{V} = 0$  at the post fault stable equilibrium point (s.e.p). The time derivative of (11) along the trajectory of (10) is given by

$$\dot{\mathcal{V}} = \text{grad}(\mathcal{V}) \cdot f_c(x) = -D(\omega - \omega_s)^2 \leq 0 \quad (12)$$

Thus, the energy function (11) is a Lyapunov function candidate for system (10). Having a CSD in the system, ( $x_s$  is neglected for UPFC and QBT),  $\bar{V}' = V + \bar{V}_{se}$  then  $P_e = \text{real}(jb\bar{E}'(\bar{E}' - \bar{V}')^*)$ . Thus, the following post fault dynamics are given:

**UPFC:**

$$\dot{x} = f_c(x) + u_1 f_{UP1}(x) + u_2 f_{UP2}(x) \quad (13)$$

**QBT:**

$$\dot{x} = f_c(x) + u f_{QBT}(x) \quad (14)$$

**CSC:**

$$\dot{x} = f_c(x) + u_c f_{CSC}(x) \quad (15)$$

where

$$f_{UP1}(x) = f_{CSC}(x) = \begin{bmatrix} 0 & -c_1 \sin \delta \end{bmatrix}^T$$

$$f_{UP2}(x) = f_{QBT}(x) = \begin{bmatrix} 0 & c_1 \cos \delta \end{bmatrix}^T$$

$$c_1 = bE'V / M$$

Using (11) as a Lyapunov function candidate for systems (13)-(15), then we have for

**UPFC:**

$$\dot{V} = \text{grad}(V) \cdot (f_c(x) + u_1 f_{UP1}(x) + u_2 f_{UP2}(x)) \leq u_1 \text{grad}(V) \cdot f_{UP1}(x) + u_2 \text{grad}(V) \cdot f_{UP2}(x) \quad (16)$$

**QBT:**

$$\dot{V} = \text{grad}(V) \cdot (f_c(x) + u f_{QBT}(x)) \leq u \text{grad}(V) \cdot f_{QBT}(x) \quad (17)$$

**CSC:**

$$\dot{V} = \text{grad}(V) \cdot (f_c(x) + u_c f_{CSC}(x)) \leq u_c \text{grad}(V) \cdot f_{CSC}(x) \quad (18)$$

By virtue of Jurdjevic-Quinn approach the following stabilizing control laws are given

**UPFC:**

$$u_1(x) = -\text{grad}(V) \cdot f_{UP1}(x) = -k_1 \sin(\delta) \dot{\delta} \quad (19)$$

$$u_2(x) = -\text{grad}(V) \cdot f_{UP2}(x) = -k_2 \cos(\delta) \dot{\delta}$$

**QBT:**

$$u(x) = -\text{grad}(V) \cdot f_{QBT}(x) = -k_3 \cos(\delta) \dot{\delta} \quad (20)$$

**CSC:**

$$u_c(x) = -\text{grad}(V) \cdot f_{CSC}(x) = k_4 \sin(\delta) \dot{\delta} \quad (21)$$

which make (16)-(18) negative. Therefore, the energy function (11) becomes a CLF for systems (13)-(15).

$k_1 - k_4$  are positive constants which are chosen individually to obtain appropriate damping.

Fig. 7 shows the stability boundary of the post fault s.e.p for the SMIB system without CSD and with CSD. The CSD are controlled by control laws (19)-(21), respectively. Fig. 7 shows that the region of stability of the post fault s.e.p is significantly enlarged by the CLF controlled CSD. Without a CSD, at fault clearing the system state lies outside the corresponding stability region. Therefore, the system is unstable for the proposed fault, see Fig. 8. However CSDs ensure that the post fault system state lies in the corresponding enlarged stability region. The controlled system is therefore stable for the proposed fault, see Fig. 8.

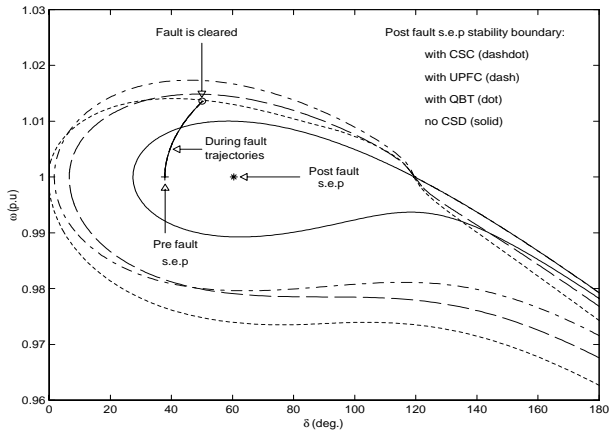


Fig. 7: Phase portrait of the SMIB system during fault

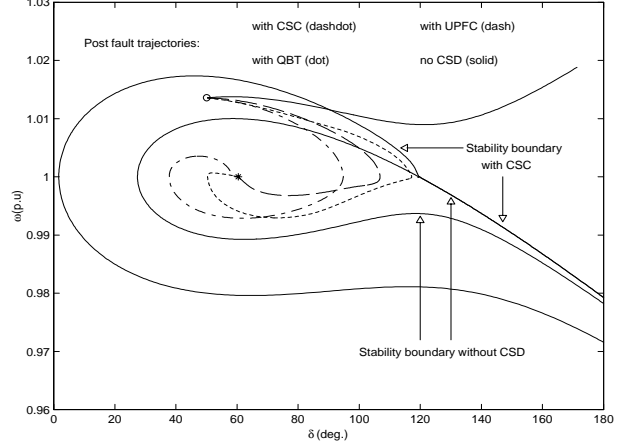


Fig. 8: Phase portrait of the SMIB system after fault

To summarize, just as the existence of a Lyapunov function is necessary and sufficient for the stability of a system without inputs, the existence of a CLF is necessary and sufficient for the stabilizability of a system with a control input [5].

### 3.2 APPLICATION IN POWER SYSTEM

Consider a power network which is modeled by  $2n + N$  nodes connected by lossless transmission lines which is represented by node admittance matrix  $Y = j[B_{kl}]$ . The first  $n$  nodes are the internal buses of the generators. The nodes  $n + 1$  to  $2n$  are the terminal buses of the generators where there may also be loads. Each generator terminal bus is connected with its internal bus through a lossless line with reactance equal to  $X'_d$ , i.e. the generator transient reactance, see Fig. 9. The remaining  $N$  nodes are the load buses. It is assumed that the mechanical input power of the generator is constant. The machine model considered here is flux-decay model (one-axis model). Exciters and governors are not included in this model.

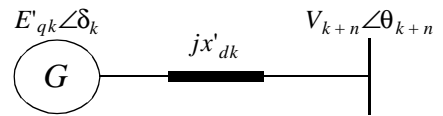


Fig. 9: Transient equivalent circuit of a generator

The rest of the treatment follows that in [8] and references therein where more details are given. The dynamics of the generators are described by the following differential equations (with respect to the COI reference frame). For  $k = 1 \dots n$

$$\begin{aligned} \dot{\delta}_k &= \tilde{\omega}_k \\ M_k \dot{\tilde{\omega}}_k &= P_{mk} - P_{ek} - D_k \tilde{\omega}_k - \frac{M_k}{M_T} P_{COI} \\ T'_{dk} \dot{E}'_{qk} &= \frac{X_{dk} - X'_{dk}}{X'_{dk}} V_{k+n} \cos(\delta_k - \theta_{k+n}) \\ &\quad + E'_{fdk} - \frac{X_{dk}}{X'_{dk}} E'_{qk} \end{aligned} \quad (22)$$

where  $P_{COI} = \sum_{k=1}^n (P_{mk} - P_{ek})$  and  $P_{ek}$  is the generated electrical power.

For the lossless system the following equations can be written at bus  $k$  where  $P_k$  is the real power and  $Q_k$  is the reactive power injected into the system from bus  $k$ .

For  $k = (2n+1) \cdots (2n+N)$

$$P_k = \sum_{l=n+1}^{2n+N} B_{kl} V_k V_l \sin(\theta_k - \theta_l)$$

$$Q_k = - \sum_{l=n+1}^{2n+N} B_{kl} V_k V_l \cos(\theta_k - \theta_l)$$

For  $k = (n+1) \cdots 2n$ ,  $P_k$  and  $Q_k$  are similar, but also take account of generated real and reactive power [8].

Real load at each bus is represented by a constant load and reactive load by an arbitrary function of voltage at the respective bus. Thus, for  $k = (n+1) \cdots (2n+N)$

$$P_{Lk} = P_{Lk}^o$$

$$Q_{Lk} = f_{qk}(V_k)$$

Therefore, for  $k = (n+1) \cdots (2n+N)$  the power flow equations can be written as

$$P_k + P_{Lk} = 0$$

$$Q_k + Q_{Lk} = 0 \quad (23)$$

An energy function for the differential algebraic equations (22) and (23), is given by

$$\mathcal{V}(\tilde{\omega}, \tilde{\delta}, E'_q, V, \tilde{\theta}) = \mathcal{V}_1 + \sum_{k=1}^8 \mathcal{V}_{2k} + C. \quad (24)$$

where

$$\mathcal{V}_1 = \frac{1}{2} \sum_{k=1}^n M_k \tilde{\omega}_k^2, \quad \mathcal{V}_{21} = - \sum_{k=1}^n P_{mk} \tilde{\delta}_k$$

$$\mathcal{V}_{22} = \sum_{k=n+1}^{2n+N} P_{Lk} \tilde{\theta}_k, \quad \mathcal{V}_{23} = \sum_{k=n+1}^{2n+N} \int \frac{Q_{Lk}}{V_k} dV_k$$

$$\mathcal{V}_{24} = \sum_{k=n+1}^{2n+N} \frac{1}{2X'_{dk-n}} (E_{qk-n}^{\prime 2} + V_k^2 - 2E'_{qk-n} V_k \cos(\delta_{k-n} - \theta_k))$$

$$\mathcal{V}_{25} = - \frac{1}{2} \sum_{k=n+1}^{2n+N} \sum_{l=n+1}^{2n+N} B_{kl} V_k V_l \cos(\theta_k - \theta_l)$$

$$\mathcal{V}_{26} = \sum_{k=n+1}^{2n} \frac{X'_{dk-n} - X_{qk-n}}{4X'_{dk-n} X_{qk-n}} (V_k^2 - V_k^2 \cos(2(\delta_{k-n} - \theta_k)))$$

$$\mathcal{V}_{27} = - \sum_{k=1}^n \frac{E_{fdk} E'_{qk}}{X_{dk} - X'_{dk}}, \quad \mathcal{V}_{28} = \sum_{k=1}^n \frac{E_{qk}^{\prime 2}}{2(X_{dk} - X'_{dk})}$$

$\mathcal{V}_1$  is known as the kinetic energy and  $\sum \mathcal{V}_{2k}$  as the potential energy.  $C$  is a constant such that at the post fault s.e.p the energy function is zero.

Using the notation  $\left[ \frac{d\mathcal{V}}{dt} \right]_{\tilde{\omega}}$  for  $\left[ \frac{d\mathcal{V}}{d\tilde{\omega}} \frac{d\tilde{\omega}}{dt} \right]$ , and similarly for the other states, then we have

$$\left[ \frac{d\mathcal{V}}{dt} \right]_{\tilde{\omega}} + \left[ \frac{d\mathcal{V}}{dt} + \frac{d\mathcal{V}}{dt} + \frac{d\mathcal{V}}{dt} + \frac{d\mathcal{V}}{dt} \right]_{\tilde{\delta}} = - \sum_{k=1}^n D_k \tilde{\omega}_k^2 \quad (25)$$

$$\left[ \frac{d\mathcal{V}}{dt} + \frac{d\mathcal{V}}{dt} + \frac{d\mathcal{V}}{dt} + \frac{d\mathcal{V}}{dt} \right]_{\tilde{\theta}} = \sum (P_k + P_{Lk}) \dot{\tilde{\theta}}_k = 0 \quad (26)$$

$$\left[ \frac{d\mathcal{V}}{dt} + \frac{d\mathcal{V}}{dt} + \frac{d\mathcal{V}}{dt} + \frac{d\mathcal{V}}{dt} \right]_V = \sum (Q_k + Q_{Lk}) \frac{\dot{V}_k}{V_k} = 0 \quad (27)$$

$$\left[ \frac{d\mathcal{V}}{dt} + \frac{d\mathcal{V}}{dt} + \frac{d\mathcal{V}}{dt} \right]_{E'_q} = - \sum_{k=1}^n \frac{T'_{dok}}{X_{dk} - X'_{dk}} (\dot{E}'_{qk})^2 \quad (28)$$

Thus, the time derivative of the energy function is

$$\frac{d\mathcal{V}}{dt} = - \sum_{k=1}^n D_k \tilde{\omega}_k^2 - \sum_{k=1}^n \frac{T'_{dok}}{X_{dk} - X'_{dk}} (\dot{E}'_{qk})^2 = \dot{\mathcal{V}}_{NOCS D} \leq 0 \quad (29)$$

Now assume that a CSD is located between buses  $i$  and  $j$  in the transmission system. The introduction of the CSD does not alter the energy function (24). However it does alter  $\dot{\mathcal{V}}$ , in particular the terms (26) and (27) no longer sum to zero. To see this, consider the  $i$ -th term of (26), i.e.  $(P_i + P_{Li}) \dot{\tilde{\theta}}_i$ . Without a CSD connected to bus  $i$ ,  $(P_i + P_{Li}) = 0$ , resulting in the zero summation of (26). However when the CSD is connected, power balance gives  $(P_i + P_{Li} + P_{si}) = 0$ . Therefore, with the CSD connected, the  $i$ -th term of (26) becomes  $(P_i + P_{Li}) \dot{\tilde{\theta}}_i = -P_{si} \dot{\tilde{\theta}}_i$ . A similar argument follows for the  $j$ -th term of (26) and the corresponding terms of (27) resulting in

$$\left[ \frac{d\mathcal{V}}{dt} + \frac{d\mathcal{V}}{dt} + \frac{d\mathcal{V}}{dt} + \frac{d\mathcal{V}}{dt} \right]_{\tilde{\theta}} = -P_{si} \dot{\tilde{\theta}}_i - P_{sj} \dot{\tilde{\theta}}_j \quad (30)$$

$$\left[ \frac{d\mathcal{V}}{dt} + \frac{d\mathcal{V}}{dt} + \frac{d\mathcal{V}}{dt} + \frac{d\mathcal{V}}{dt} \right]_V = -Q_{si} \frac{\dot{V}_i}{V_i} - Q_{sj} \frac{\dot{V}_j}{V_j} \quad (31)$$

Note that (25) and (28) are unaffected by the introduction of a CSD.

Therefore, the time derivative of the energy function along the trajectories of the system with CSD becomes

$$\frac{dV}{dt} = \dot{V}_{NOCS D} + \dot{V}_{CSD} \leq \dot{V}_{CSD} \quad (32)$$

Simplification of  $\dot{V}_{CSD}$  for various devices gives

**UPFC:**

$$\dot{V}_{CSD} = -b_s V_i \left[ u_1 \frac{d}{dt} (V_i - V_j \cos(\theta_{ij})) + u_2 \frac{d}{dt} (V_j \sin(\theta_{ij})) \right]$$

**QBT:**

$$\begin{aligned} \dot{V}_{CSD} &= -b_s \left[ u \frac{d}{dt} (V_i V_j \sin(\theta_{ij})) + \frac{1}{2} u^2 \frac{d}{dt} V_i^2 \right] \\ &\approx -b_s u \frac{d}{dt} (V_i V_j \sin(\theta_{ij})) \end{aligned}$$

**CSC:**

$$\begin{aligned} \dot{V}_{CSD} &= -\frac{1}{2} b_s u_c \frac{d}{dt} [V_i^2 + V_j^2 - 2V_i V_j \cos(\theta_{ij})] \\ &= -\frac{1}{2} b_s u_c \frac{d}{dt} |\bar{V}_{ij}|^2 = -\frac{1}{2} b_s u_c \frac{d}{dt} [x_L I_{csc} - V_{csc}]^2 \end{aligned}$$

where,  $I_{CSC}$  is absolute value of current through CSC and  $V_{CSC}$  is absolute value of voltage over CSC.

The energy function will be a CLF, if  $\dot{V}_{CSD}$  is negative. Therefore, the following control (feedback) laws are suggested, (note that  $V_i$  and  $b_s$  are positive):

**Control law for UPFC:**

$$\begin{aligned} u_1 &= k_1 \frac{d}{dt} (V_i - V_j \cos(\theta_{ij})) \\ u_2 &= k_2 \frac{d}{dt} (V_j \sin(\theta_{ij})) \end{aligned} \quad (33)$$

**Control law for QBT:**

$$u = k_3 \frac{d}{dt} (V_i V_j \sin(\theta_{ij})) \quad (34)$$

**Control law for CSC:**

$$u_c = k_4 \frac{d}{dt} [x_L I_{csc} - V_{csc}]^2 \quad (35)$$

where,  $k_1, k_2, k_3$  and  $k_4$  are positive constants which are chosen individually to obtain appropriate damping.

For CSC,  $u_c$  and  $x_c$  have the same sign, see (2). Therefore,  $u_c$  can be replaced by  $x_c$  in (35), i.e.

$$x_c = k_5 \frac{d}{dt} [x_L I_{csc} - V_{csc}]^2 \quad (36)$$

Note that each individual CSC contributes a  $\dot{V}_{CSD}$  term to  $\frac{dV}{dt}$ . If there are a number of CSCs in the system, the overall contribution is the sum of the individual terms. All CSC models have  $P_{si} = -P_{sj}$ . This allows (32) to be written

$$\begin{aligned} \frac{dV}{dt} &= \dot{V}_{NOCS D} + \dot{V}_{CSD} \leq \dot{V}_{CSD} \\ &= -P_{si} \dot{\theta}_{ij} - Q_{si} \frac{\dot{V}_i}{V_i} - Q_{sj} \frac{\dot{V}_j}{V_j} \end{aligned} \quad (37)$$

This is always valid, irrespective of the generator and load models used in the development of the various energy functions in [8]. Different models contribute different terms to the left-hand sides of (30) and (31), but the right hand sides remain unchanged. Thus the control laws based on the CLF rely only on locally measurable information and are independent of system topology and modeling of power system components. Also, these control laws do not require knowledge of post fault stable equilibrium point.

Similar analysis can be found in [9]-[10]. For example, using the classical generator model and assuming constant voltages at all buses, the contribution to  $\dot{V}$  of (31) is zero. The control law for a CSC, given by (35), becomes  $u_c = kb_s V_i V_j \sin(\theta_{ij}) \dot{\theta}_{ij} = k_4 \sin(\theta_{ij}) \dot{\theta}_{ij}$  which is similar to the control law suggested in [10], with the exceptions that it is not a discrete control law and does not require the post fault stable equilibrium point, i.e.  $P_{ko}$  in [10].

## 4. NUMERICAL EXAMPLE

In this section, various test systems will be used for applying the control laws (33)-(35). Note that these control laws were developed assuming classical Lyapunov modeling, but they will be applied in the examples to 'real' systems that are not subject to those modeling restrictions. In the following test systems, the active and reactive components of loads have constant current and constant impedance characteristics, respectively. Also, if not otherwise stated, the exact data and generator modeling from the corresponding given references are used.

All simulation are performed by using SIMPOW [11] and the results are plotted in MATLAB.

### 4.1 TEST SYSTEM I (Two-area system)

Fig. 10 shows a simple two-area system. The system data and generator modeling can be found in [12]. A three-phase fault occurs at point F. The fault is cleared after 100 ms by opening of the faulted line.

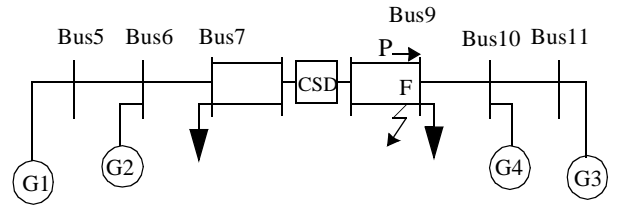


Fig. 10: Two-area system

All generators include thyristor excitation system without PSS with  $T_R = T_A = 0$ ,  $K_A = 300$  and  $T_B = 0.01$ , see Fig. E12.9 in [12]. Two loading cases are considered. In case 1,  $P_{G1} = P_{G2} = 700$  MW and in case 2,  $P_{G1} = P_{G2} = 730$  MW.

For UPFC  $r_{max} = 0.094 pu$ , for QBT  $r_{max} = 0.1 pu$  and for CSC  $0 \leq x_c \leq 25 \Omega$ .

Fig. 11 shows variation of  $P$  vs. time.  $P$  is the real power through the unfaulted line between the CSD and bus 9, see Fig. 10. The solid curves in Fig. 11 show  $P$  when there was no CSD. The dotted, dashed and dash-dotted curves show  $P$  for CLF control of a UPFC, QBT and CSC, respectively. The simulation results show the ability of the control laws to stabilize and damp the two-area power system for proposed fault and cases.

Case 2 shows clearly that the CSDs which are controlled by the CLF, enlarge stability region.

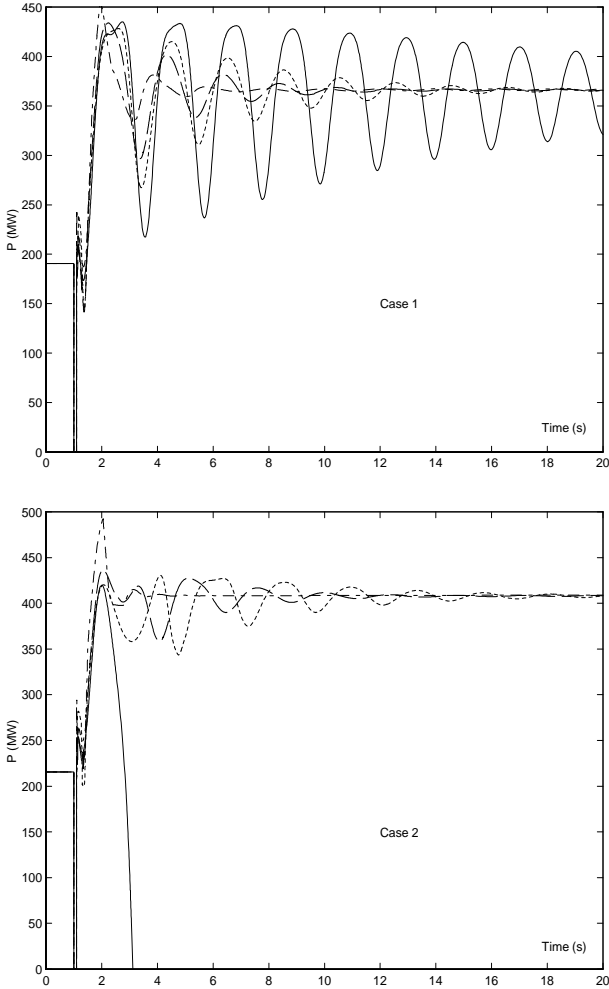


Fig. 11: Variation of power through unfaulted line,  $P$ , vs. time in two-area system

#### 4.2 TEST SYSTEM II (IEEE 9 bus test system)

Fig. 12 shows the IEEE 9 bus test system. The system data can be found in [13]. In this example and following examples, it will be shown that the multi CLF controlled CSDs do not adversely affect each other. Indeed, they improve damping of the electromechanical oscillations. A three-phase fault occurs at bus4. The fault is cleared after 100 ms. No line is tripped. Fig. 13 shows variation of  $P$  identified in Fig. 12. A QBT, UPFC and CSC, respectively, are installed in the line between bus 9 and bus 6 and also a CSC, say CSC1, is installed in the line between bus 7 and bus 5.

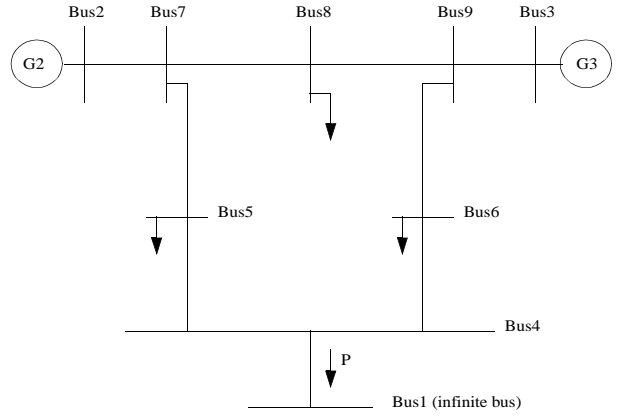


Fig. 12: IEEE 9 bus system

The solid curves in Fig. 13 show variation of  $P$  when there was no CSD. The dotted, dash and dash-dotted curves show  $P$  for CLF control of a QBT, UPFC and CSC, respectively without CSC1 (upper figure) and

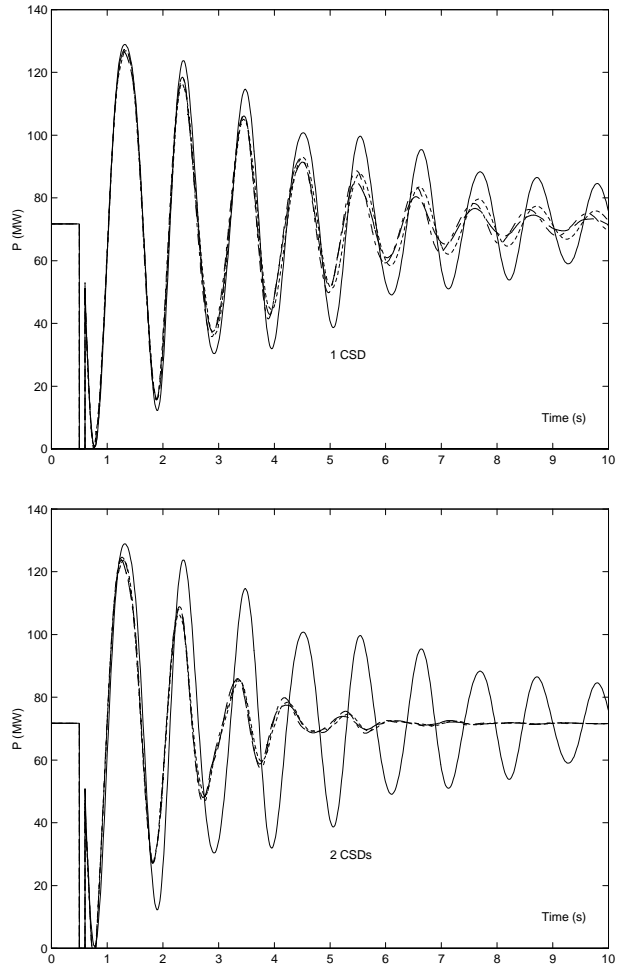


Fig. 13: Variation of  $P$  (power between buses 4 and 1) vs. time in IEEE 9 bus system

The CSDs have the following data:  
for UPFC  $r_{\max} = 0.013$  and for QBT  $r_{\max} = 0.012 \text{ p.u.}$   
for CSC  $0 \leq x_c \leq 0.04$  and CSC1  $0 \leq x_c \leq 0.05 \text{ p.u.}$

### 4.3 TEST SYSTEM III (Nordic32A test system)

Nordic32A is a test system for simulation of transient stability and long term dynamics proposed by CIGRE Task Force 38.02.08 [14]. The exact data from [14] is used with the exception that no PSS is used in the system. The system contains 32 high voltage buses. The main transmission system is designed for 400 kV. There are also some regional systems at 220 kV and 130 kV. Both hydro power plants and thermal power plants with a total of 23 generators are modeled. The hydro power plants are located in the North and External regions of the system and are equipped with salient pole generators whose models include models of AVR, saturation, one field winding, one damper winding in d-axis and one damper winding in q-axis. The thermal power plants are located in the Central and South regions and each plant includes a round rotor generator whose model includes all features included in the salient pole model but also a second damper winding in q-axis and saturation in the resulting air-gap flux. Only the hydropower units are using governors. The generators have no inherent damping, i.e. the damping constant  $D$  is zero.

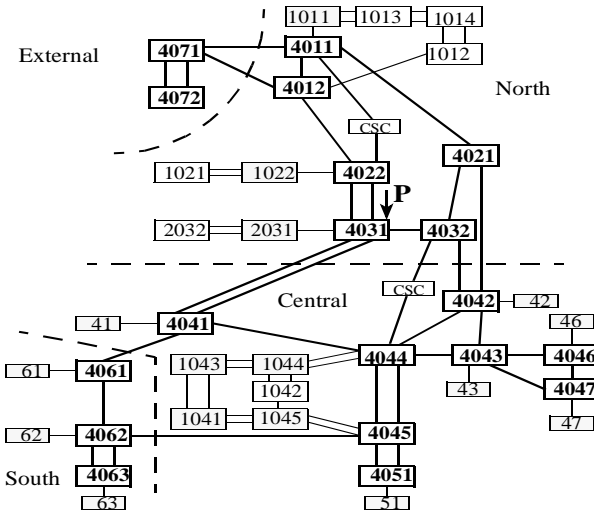


Fig. 14: Nordic32A test system proposed by CIGRE

Two loading cases are considered, namely LF32-028 and LF32-029. In LF32-028, the transfers are high from North to Central. The load level is at peak load. The case is sensitive to many types of faults. In fact the transfer situation is above that recommended by normal security standards. LF32-029 is similar to LF32-028 but transfers from North to Central are decreased. It is made by an extra generation at bus 4051 and a decreasing of generating powers in some generators in North. Two CSCs are used in the system. The first CSC is located in line 4011-4022 and the second one in line 4032-4044. The steady state set points of both CSCs are  $12.8 \Omega$ .

For the first CSC,  $8 \leq x_c \leq 30 \Omega$  and for the second one  $8 \leq x_c \leq 20 \Omega$ . Various faults and contingencies have been studied for both LF32-028 and LF32-029. For all cases the CLF controlled CSCs damped power oscillations in an effective and robust manner. Also, various

load characteristics were applied for this system and simulation results showed that the damping effect of the CLF controlled CSCs was not sensitive to the load modeling. In this paper, we only show the simulation results of one case, that is a three-phase fault imposed on transmission line 4011-4021 at a position very close to bus 4021. The fault is cleared by disconnecting both ends of line 4011-4021 after 100 ms.

In Fig. 15, the solid and dash-dotted curves show variation of  $P$ , identified in Fig. 14, when the CSCs are uncontrolled, and controlled using CLF, respectively.

Note that these two CLF controlled CSCs do not adversely affect each other. The reason is that each device contributes to make the time derivative of the energy function negative.

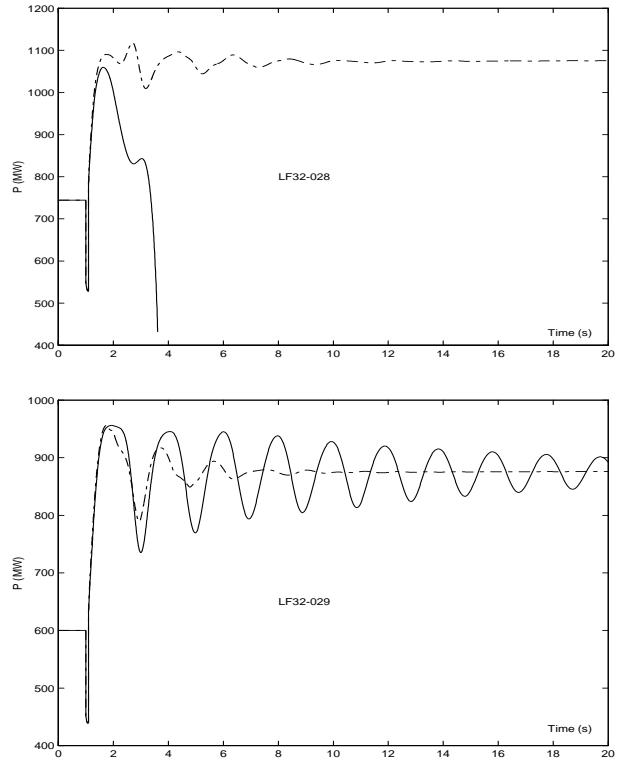


Fig. 15: Variation of  $P$  (power through one of the lines between buses 4022 and 4031) vs. time in Nordic32A system

### 4.4 TEST SYSTEM IV (Brazilian network)

Fig. 16 shows the Brazilian network described in [15]. The North/Northeast interconnected system consists of large hydro-generating complexes that are linked to 230 and 500 kV transmission networks.

The South/Southeast/Midwest interconnected system consists of a large number of hydro-generating plants linked to the main load centers by transmission networks operating in the 138 and 750 kV. The North-South interconnect transmission line is 1028 km with a circuit rating of 1300 MW. Full details are given in [15]. Two cases are studied in this paper. In case1, a fault occurs in the Northeast system. The fault is cleared after 100 ms. No line is tripped. In case2, a generator is tripped in the South system.

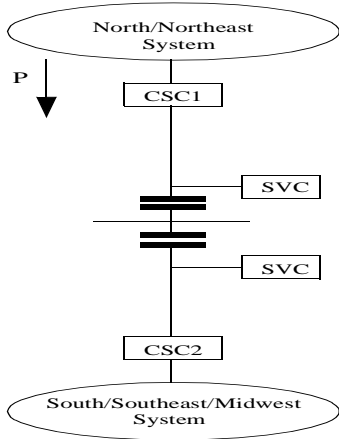


Fig. 16: Brazilian network

Fig. 17 shows variation of  $P$  identified in Fig. 16 for the two cases. The steady state set points of both CSC are  $15.84 \Omega$  and for both CSCs  $13.2 \leq x_c \leq 40 \Omega$ .

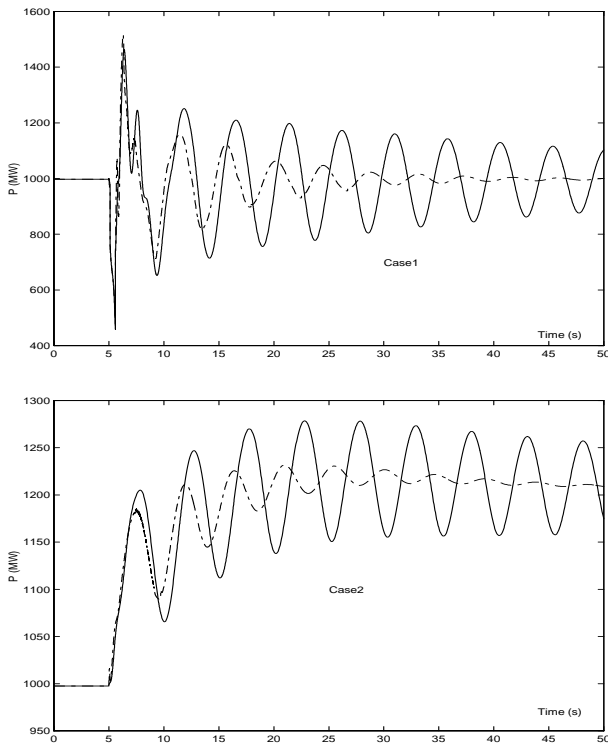


Fig. 17: Variation of  $P$  vs. time in Brazilian network

The solid curves in Fig. 17 show  $P$  when CSCs are not controlled and the dash-dotted curves when CSCs are controlled by CLF.

## 5. DISCUSSION AND FUTURE WORK

In Nordic32A test system and Brazilian network, both CSCs have steady state set points, that is each CSC is defined by  $x_c = x_{co} + \Delta x_c$ , where  $x_{co}$  is the steady state set point and  $\Delta x_c$  is the control modulation which is controlled by the CLF control law. Since  $x_{co}$  is a constant, the reactance of the line in which the CSC is installed, can be given by  $x_s = x_L^{new} = x_L - x_{co}$ .

Thus,  $x_c$  in (36) is replaced by  $\Delta x_c$ .

A question of importance is the selection of the constants  $k_1 - k_5$  in the control laws (33)-(36). Mathematically, any positive  $k_1 - k_5$  should stabilize the system as long as the trajectories lie inside the (enlarged) stability region. In practice, there are limitations for those constants. To see that, we use SIME which assesses the behavior of a power system in its post fault configuration in terms of a generalized One Machine Infinite Bus (OMIB) transformation [16]. Now, consider the two-area system with the same CSC data and the same fault but  $P_{G1} = P_{G2} = 750 MW$ . Fig. 18 shows the phase portrait of the generalized OMIB of the two-area system for various values of  $k_5$ .

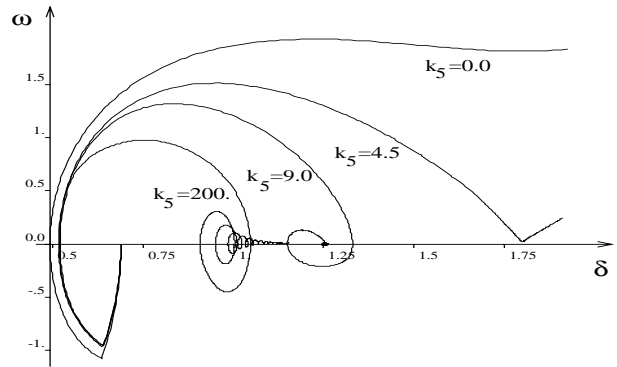


Fig. 18: Phase portrait of the generalized OMIB of the two-area system for various  $k_5$

For  $0 < k_5 \leq 4.5$ , the enlargement of the region of stability by CSC is not large enough for having the trajectories inside the enlarged stability region when the proposed fault is cleared, but it dose for  $k_5 > 4.5$ . For around  $k_5 = 9$ , the system is well damped and the trajectories rapidly go towards the post fault s.e.p. For large  $k_5$ , the system is still stable, but the trajectories slowly go towards the post fault s.e.p.

The model used in the development of the control laws (33)-(35) had a very specific form. It was convenient for obtaining a Lyapunov function, but only approximately describes actual power system behavior. The issue of modeling approximations, and their influence on the stabilization of power systems, is yet to be fully addressed. It is an important focus of the authors' current research. The model (3) will be used to illustrate these ideas.

Assume that the model used in the development of the CLF has the form

$$\dot{x} = f^*(x) \quad (38)$$

whereas the actual system is described by  $\dot{x} = F(x)$ .

Simple manipulation gives

$$\dot{x} = F(x) + f^*(x) - f^*(x) = f^*(x) + p(x) \quad (39)$$

Since it is difficult to find a Lyapunov function for (39), a Lyapunov function is derived for (38), i.e. when  $p(x) = 0$ , and a control law established which makes that Lyapunov function a CLF. The following questions

arise. How does this control law, derived for (38), affect  $p(x)$ ? In the context of CSD control, how good are the control laws (33)-(35) when the system is lossy, and more detailed models are used for generators and loads? The simulation results in this paper, and from various other studies, provide a partial answer. They indicate that the control laws are not sensitive to the model approximations. However it is important to obtain an analytical justification of this observation. Theorem 5.3 and the concept of total stability in [2] may provide a partial answer. It remains to extend these theorems to differential algebraic systems.

## 6. CONCLUSIONS

It has been shown that the Controllable Series Devices (CSD) provide an effective means of adding damping to power systems and significantly enlarge the region of stability of the post fault stable equilibrium point. Also, control laws for CSDs based on Control Lyapunov function (CLF) concepts have been derived. The control laws rely only on locally measurable information and are independent of system topology and modeling of power system components. For these control laws, knowledge of post fault stable equilibrium points is not required. Finally, it has also been shown that CSDs with CLF control do not adversely affect each other.

## 7. ACKNOWLEDGEMENTS

The authors gratefully acknowledge numerous useful comments by M. Noroozian, L. Ängquist and B. Berggren of ABB, M. Danielsson of Svenska Kraftnät, Jim Gronquist of PG & E and Damien Ernst of University of Liege in Belgium. Also, financial support from ABB and Svenska Kraftnät through the Elektra program is gratefully acknowledged.

## 8. BIOGRAPHIES

**Mehrdad Ghandhari** (S'99) received his M.Sc. and Tech.Lic degrees in electrical engineering from Royal Institute of Technology, Sweden in 1995 and 1997, respectively. He is currently pursuing graduate studies at the Royal Institute of Technology.

**Göran Andersson** (M'86, SM'91, F'97) received his M.Sc. and Ph.D. degrees from the University of Lund in 1975 and 1980, respectively. In 1980, he joined ASEA's HVDC--division and in 1986 he was appointed professor in Electric Power Systems at the Royal Institute of Technology, Sweden. He is a member of the Royal Swedish Academy of Engineering Sciences and the Royal Swedish Academy of Sciences.

**Ian A. Hiskens** (S'77, M'80, SM'96) received the BEng and BAppSc(Math) degrees from the Capricornia Institute of Advanced Education, Rockhampton, Australia in 1980 and 1983, respectively. He received his Ph.D. degree from the University of Newcastle, Australia in

1990. He was with the Queensland Electricity Supply Industry 1980-1992 and the University of Newcastle 1992-1999. He is currently a Visiting Associate Professor at the University of Illinois at Urbana-Champaign.

## 9. BIBLIOGRAPHY

- [1] L. Gyugyi, et al., "The Unified Power Flow Controller: A new approach to Power Transmission Control", IEEE Trans. Power Delivery, vol. 10, no. 2, April 1995, pp. 1085-1097.
- [2] H. K. Khalil, Nonlinear Systems (second edition), Prentice-Hall, Inc., 1996.
- [3] Z. Artstein, "Stabilization with relaxed controls", Nonlinear Analysis, Theory, Methods and Applications, vol. 7, no. 11, 1983, pp. 1163-1173.
- [4] E. Sontag, "A universal construction of Artstein's theorem on nonlinear stabilization", Systems and Control Letters 13, 1983, pp. 1163-1173.
- [5] R. A. Freeman and P. V. Kokotovic, Robust Nonlinear Control Design, Birkhäuser, 1996.
- [6] A. Bacciotti, Local Stabilizability of Nonlinear Control Systems, World Scientific Publishing Co. Pte. Ltd., 1996.
- [7] V. Jurdjevic and J. P. Quinn, "Controllability and Stability", Journal of Differential Equations 28, 1978, pp. 381-389.
- [8] M. A. Pai, Energy Function Analysis for Power System Stability, Kluwer Academic Publishers, 1989.
- [9] J. F. Gronquist et al., "Power Oscillation Damping Control Strategies for FACTS Devices Using Locally Measurable Quantities", IEEE, Trans. on Power Systems, vol. 10, no. 3, 1995, pp. 1598-1605.
- [10] K R Padiyar and K Uma Rao, "Discrete control of series compensation for stability improvement in power systems", International Journal of Electrical Power & Energy Systems, vol. 19, no. 5, 1997, pp. 311-319.
- [11] H. R. Fankhauser et al., "SIMPOW- a digital power system simulator", ABB Review, no. 7, 1990.
- [12] P. Kundur, Power System Stability and Control, McGraw-Hill, 1994.
- [13] P. M. Andersson and A. A. Fouad, Power system control and stability, Vol. 1. Ames, IA: The Iowa State Univ. Press, 1977.
- [14] CIGRE Task Force 38.02.08, "Longer term dynamics phase II", Final report, January 1995.
- [15] B. Carraro and J. Salomao, "Power Corridor Unites Brazil's Network", Transmission and Distribution World, June 1999, pp. 70-74.
- [16] Y. Zhang, et al., "SIME: A hybrid Approach to Fast Transient Stability Assessment and Contingency Selection", International Journal of Electrical Power & Energy Systems, Vol. 19, No. 3, 1997, pp. 195-208.